AD

TECHNICAL REPORT BRL-TR-2864

HAN-BASED LIQUID GUN PROPELLANTS: PHYSICAL PROPERTIES

MADELYN M. DECKER, NATHAN KLEIN
ELI FREEDMAN, CHARLES S. LEVERITT
JOSEPHINE Q. WOJCIECHOWSKI

NOVEMBER 1987

US ARMY BALLISTIC RESEARCH LABORATORY
ABERDEEN PROVING GROUND, MARYLAND

DESTRUCTION NOTICE

Destroy this report when it is no longer needed. DO NOT return it to the originator.

Additional copies of this report may be obtained from the National Technical Information Service, U.S. Department of Commerce, Springfield, VA 22161.

The findings of this report are not to be construed as an official Department of the Army position, unless so designated by other authorized documents.

The use of trade names or manufacturers' names in this report does not constitute indorsement of any commercial product.

UNCLASSIFIED

SECURITY CLASSIFICATION OF THIS PAGE

AD-A195 246

REPORT DOCUMENTATION PAGE

Form Approved
OMB No 0704-0188
Exp Date Jun 30, 1986

1a REPORT SECURITY CLASSIFICATION: Unclassified	1b RESTRICTIVE MARKINGS
2a SECURITY CLASSIFICATION AUTHORITY	3 DISTRIBUTION / AVAILABILITY OF REPORT
2b DECLASSIFICATION / DOWNGRADING SCHEDULE	
4 PERFORMING ORGANIZATION REPORT NUMBER(S): BRL-TR-2864	5 MONITORING ORGANIZATION REPORT NUMBER(S)
6a NAME OF PERFORMING ORGANIZATION: US Army Ballistic Rsch Lab; 6b OFFICE SYMBOL (If applicable): SLCBR-IB	7a NAME OF MONITORING ORGANIZATION
6c ADDRESS (City, State, and ZIP Code): Aberdeen Proving Ground, MD 21005-5066	7b ADDRESS (City, State, and ZIP Code)
8a NAME OF FUNDING / SPONSORING ORGANIZATION; 8b OFFICE SYMBOL (If applicable)	9 PROCUREMENT INSTRUMENT IDENTIFICATION NUMBER
8c ADDRESS (City, State, and ZIP Code)	10 SOURCE OF FUNDING NUMBERS: PROGRAM ELEMENT NO. / PROJECT NO. / TASK NO. / WORK UNIT ACCESSION NO

11 TITLE (Include Security Classification)
HAN-Based Liquid Gun Propellants: Physical Properties

12 PERSONAL AUTHOR(S)
Decker, Madelyn M., Freedman, Eli, Klein, Nathan, Leveritt, Charles S., Wojciechowski, J.Q.

13a TYPE OF REPORT	13b TIME COVERED	14 DATE OF REPORT (Year, Month, Day)	15 PAGE COUNT
Final	FROM _____ TO _____		

16 SUPPLEMENTARY NOTATION

17 COSATI CODES		
FIELD	GROUP	SUB-GROUP

18 SUBJECT TERMS (Continue on reverse if necessary and identify by block number)
Liquid Propellants, Hydroxylammonium Nitrate, Density, Vapor Pressure, Viscosity, Surface Tension, 1845, 1846, Low Temperature, Conductivity, Equation of State, HAN

19 ABSTRACT (Continue on reverse if necessary and identify by block number)

Mixtures of hydroxylammonium nitrate (HAN), water, and the nitrate salt of an aliphatic amine (AAN), are being actively considered as propellants for use in a liquid propellant gun. A number of such AAN salts have been considered for this application; the preferred one is triethanolammonium nitrate (TEAN), which is used in propellants LGP 1845 and 1846, the current prime candidates for the gun now under development.

The physical properties of the propellants and of their components must fall within acceptable ranges for practical applications. The low temperature properties of LGP 1845 and 1846 and of HAN-water and TEAN-water mixtures have been investigated. The results for LGP 1845 and 1846 show only transitions from homogeneous liquid to homogeneous glass at -90°C and -100°C, respectively, with no indication of crystallization or component separation over wide concentration ranges. Results for HAN-water and TEAN-water mixtures are complex; crystallization, phase separation, and glass transitions are seen.

20 DISTRIBUTION / AVAILABILITY OF ABSTRACT	21 ABSTRACT SECURITY CLASSIFICATION
☐ UNCLASSIFIED/UNLIMITED ☒ SAME AS RPT ☐ DTIC USERS	Unclassified
22a NAME OF RESPONSIBLE INDIVIDUAL: Nathan Klein	22b TELEPHONE (Include Area Code): (301) 278-6173; 22c OFFICE SYMBOL: SLCBR-IB-B

DD FORM 1473, 84 MAR

83 APR edition may be used until exhausted
All other editions are obsolete

SECURITY CLASSIFICATION OF THIS PAGE
UNCLASSIFIED

18. SUBJECT TERMS (con't)

Triethanolammonium Nitrate TEAN

19. ABSTRACT (con't)

The effect of the molecular structure of the AAN on the physical properties of the propellant has also been studied. Propellants containing AANs with 0, 1, 2, or 3 hydroxyl groups were synthesized and their viscosities and densities determined as a function of temperature. The results clearly show the effects of hydrogen bonding on the physical properties.

Surface tension and vapor pressure have been determined and an equation of state that accurately describes the effect of temperature and pressure on physical properties has been developed. A model that predicts propellant properties quite adequately now exists.

ACKNOWLEDGEMENT

Many of the density, vapor pressure, and viscosity data contained in this report was obtained under contracts DAAK11-83-C-0025 and DAAA15-85-C-0116 by personnel of the Princeton Combustion Research Laboratories, Inc., Monmouth Junction, NJ, and we acknowledge the assistance and efforts of Craig A. Spiegel and Neale A. Messina of PCRL.

We thank J. Frankel and M. Doxbeck of the Benet Weapons Laboratory, Watervliet Arsenal, NY, for permitting us the use of their data in advance of its publication.

TABLE OF CONTENTS

LIST OF FIGURES

LIST OF TABLES

I. INTRODUCTION

The use of aqueous liquid propellants containing hydroxylammonium nitrate (HAN) has been discussed in several reports.[1-4]

Briefly:

* The HAN-based propellants are mixtures of HAN, water, and the nitrate salt of an aliphatic amine (AAN).

* They are formulated to be stoichiometric with respect to carbon dioxide, nitrogen, and water.

* Total energy increases with decreasing water content.

* Their thermal initiation temperatures vary inversely with nitrate-ion concentration.[5]

* The rate of gas production after initiation is related to the structure of the AAN, with the salts of tertiary amines being the best suited for use in guns.

* The most useful formulations to date are LGP 1845 and 1846, whose compositions are shown in Table 1.

TABLE 1. Propellant Compositions

Propellant	Composition					
	HAN		TEAN		Water	
	(wt %)	(M)	(wt %)	(M)	(wt %)	(M)
1845	63.23	9.62	19.96	1.38	16.81	13.64
1846	60.79	9.09	19.19	1.30	20.02	15.93

Knowledge of the low-temperature properties of these propellants is needed to ensure compliance with the requirement that all Army materiel must be operational over the temperature range from + 55°C to -55°C; therefore, it is essential that these propellants remain homogeneous liquids to at least -55°C, and that they be pumpable at this temperature; hence we need to know their viscosities as a function of temperature. In addition, knowledge of the physical properties of the propellants and their components furnishes a basis for system modeling and hence to a capability for prediction of properties under conditions where experimental measurements can be made only with difficulty or not at all; e.g., inside a gun chamber during combustion.

This report addresses the measurement and evaluation of selected properties of the propellants and their components. Both equilibrium properties such as density and vapor pressure and transport properties such as viscosity and conductivity are considered. The low temperature behavior, covering freezing points, component crystallization, and phase transitions of the propellants and their components are described. In addition, the role of the molecular structure of the AAN salt in affecting the properties of the HAN-AAN-water mixture is explored.

II. BACKGROUND

One of the most significant structural features present in HAN and TEAN is the hydroxyl group. The presence of this group in a molecule often results in hydrogen bonding which decreases vapor pressure, increases boiling point,

d enhances water miscibility. Hydrogen bonds can change physical properties by forming molecular clusters, thus raising the effective molecular weight of the compound. An example is the comparison of the kinematic viscosity of liquid propellants LGP 1845 and 1776. These formulations are quite similar in energy content, stoichiometry, and rate of energy release but differ in AAN, LGP 1776 containing trimethylammonium nitrate which lacks the hydroxyl groups of TEAN, used in LGP 1845. Measurements of kinematic viscosity under identical conditions showed[6] that LGP 1776 is less viscous than LGP 1845 over the temperature range -70 to +25°C. Results of these preliminary viscosity measurements indicated that the molecular structure of the AAN component affected the physical properties of the mixture to a significant extent, so a more complete study was warranted.

With this in mind, the role of molecular structure of the AAN component on propellant viscosity was chosen for study, this being the only component readily available for such investigation. Replacement of an hydroxyl group in TEAN by a hydrogen should significantly lower the hydrogen bonding capability of the overall system and thus decrease the molecular organization available. Every attempt was made to retain propellant characteristics other than the structure of the AAN. Thus, the mixtures prepared were all 11 molar in nitrate and were stoichiometric with respect to the formation of water, nitrogen, and carbon dioxide. Propellant nomenclature and composition are given in Table 2.

TABLE 2. Propellant Formulations

Propellant	Amine	Composition (moles/liter) HAN	AAN
0	triethylamine	9.84	1.16
1	diethylethanolamine	9.78	1.22
2	ethyldiethanolamine	9.71	1.29
3	triethanolamine	9.63	1.38

The number of hydroxyl groups in the AAN increases stepwise from 0 to 3, the nomenclature indicating the number of hydroxyl groups present in the AAN salt; propellant 3 should be identical to LGP 1845. Great care was taken in preparing the mixtures to obtain similarity in nitrate concentration within the set rather than attempting to match concentration to a particular propellant lot produced elsewhere or at another time. It is thus possible that the properties of propellant 3 differ slightly from those of LGP 1845.

III. EXPERIMENTAL METHODS

1. PROPELLANT SYNTHESIS

The four AAN salts (Table 2) were prepared by dropwise addition of the corresponding amine into 4 molar nitric acid with vigorous stirring. The acid mix was kept in an ice bath; the addition rate was such that a temperature between 0 and 5°C was maintained throughout the course of the synthesis. Reaction was considered complete when a slight excess of amine was detected in the reaction vessel.

Water was removed from the salt solution at 50°C under vacuum until crystallization began. The residue was cooled to -50°C and the crystal mass collected on a glass frit filter under vacuum. Care was taken to exclude air from the crystalline AAN salts. The salts were recrystallized from distilled water and stored in a dessicator over calcium chloride until used. Since both solution of the AAN salts and mixing of the AAN salts with HAN are endothermic, no risk of thermal decomposition is encountered during propellant formulation and the mixtures were prepared without special precautions.

2. LOW TEMPERATURE BEHAVIOR

Differential scanning calorimetry (DSC) is the experimental technique used for assessing the low-temperature properties of the propellants and their components.

All of the data were obtained using a Mettler TA 3000 Thermal Analysis System consisting of a Model TC 10A Processor and Model DSC 30 Low Temperature Cell. Samples were sealed in 100 μl glass crucibles and were referenced against similar sample crucibles filled with air, a substance that exhibits no thermal events over the temperature range studied. The glass crucibles, obtained from Mettler, are precision ground flat at the bottom to achieve good contact with the thermal sensors that generate the data. They were chosen in part because both HAN and the propellants are known to react with many metals[7] normally used as sample containers. The sealed samples could be used repeatedly because no chemical changes take place over the temperature range

studied. In addition, the transparent container enabled viewing of the samples, a matter of substantial importance in cases where a number of complex transitions were recorded. Concentrated HAN and crystalline TEAN were obtained from Morton-Thiokol Inc., Elkton Division, and used without further purification. The HAN and TEAN samples used were prepared by dilution with distilled water. Heating and cooling rates were varied, and measurements were made during both heating and cooling cycles.

HAN-water mixtures at HAN concentrations of 0.1, 0.4, 0.8, 2.0, 4.0, 8.0, 9.0, 10.0, 11.0, 12.0, 14.0, and 15.8 M were investigated over the temperature range -150 to 20°C. Comparable investigations of TEAN-water mixtures at TEAN concentrations of 0.8, 1.0, 2.0, 4.0, and 4.8 M were completed. Finally, the low temperature profiles of LGP 1845 and 1846 as well as of propellants 0, 1, 2, and 3 were obtained.

3. DENSITY

Density was measured as a function of temperature using a thermostated Mettler Model DMA 55 Density Meter. The lowest temperature obtainable with this apparatus was -10°C, a limitation imposed by the constant temperature bath used. Density values below -10°C were obtained by linear extrapolation of the experimental data. Justification for such extrapolation is based on the absence of phase transitions over the extrapolated range and the reported validity of such extrapolations.[8] At temperatures between -10 and 65°C, temperature was controlled to at least $\pm 0.1^{\circ}$. The density meter measures

variation in the natural frequency of a hollow oscillator which is related to density according to

$$\rho = (1/A)(\tau^2 - B)$$

where ρ is density (g/ml), τ is the period of the oscillation, and A and B are empirical instrument constants. The instrument was calibrated with several fluids of known density. Reported values are accurate to within 0.01%.

Additionally, the densities of HAN solutions at room temperature were measured at various concentrations of HAN using carefully calibrated (NBS traceable) hydrometers.[9]

4. EQUATION OF STATE

Data required for derivation of an equation of state were obtained by Frankel and Doxbeck[10] who measured the variation of sound velocity with pressure and temperature. Variations in density with pressure and specific heat with temperature were also determined. A complete equation of state was developed from these data.

5. SURFACE TENSION

Surface tension measurements as a function of temperature were made on LGP 1845 and 1846 with a Wilhemy Plate tensiometer.[11] Only solutions in

equilibrium with water vapor were studied.

6. VAPOR PRESSURE

Vapor pressure measurements were made using an isoteniscope.[12] Samples were degassed using a repeated freeze-pump-thaw cycle to prevent loss of solvent during the removal of dissolved gases that must precede measurement. Water loss during degassing was less than 0.6% in all cases. The apparatus and technique was tested and verified using aqueous 50 wt % $Ca(NO_3)_2$, an essentially inert mixture with known vapor pressure.[13] It was expected that the vapor pressure characteristics of this system would be similar to the propellants.

7. VISCOSITY

Viscosity of the propellants was determined using an Ubbelohde glass capillary viscometer,[14] which measures kinematic viscosity, η. Since dynamic viscosity, μ, is the quantity dealt with in analytical evaluation, the experimental data were converted using the definition

$$\mu = \eta \times \rho.$$

In general, the determination of kinematic viscosity is less sensitive to variation in experimental technique and is preferred if the data are to be applied to conditions that differ markedly from those under which the

measurements were made. Density measurements, obtained as another part of the physical properties investigation, were used to calculate μ. Measurements were made over the temperature range -55°C to 65°C. Specific details of the method used have been previously described.[15]

IV. RESULTS AND DISCUSSION

1. LOW TEMPERATURE BEHAVIOR

The low temperature data obtained with HAN-water mixtures present a fairly complex set of events. The Figures are presented in order to illustrate specific events and are not intended to convey the impression that these events suddenly appear as HAN concentration is changed. In fact, precisely the opposite is the case, the various features seen in the Figures appearing gradually, becoming dominant, and eventually becoming the only features seen.

The data show two distinct events, one at each concentration extreme. Addressing high HAN concentrations (> 11 M) first, Figure 1 is a typical DSC record taken on a sample of 14.0 M HAN, heated at a rate of 5°C/min. The heat capacity of the sample both before and after the transition appears constant and visual inspection of the sample indicates change from an opaque and apparently homogeneous solid to a homogeneous liquid. Both the shape of the curve and the change in heat capacity are characteristic of a glass transition. Crystallization is not observed and the mixtures exhibit behavior

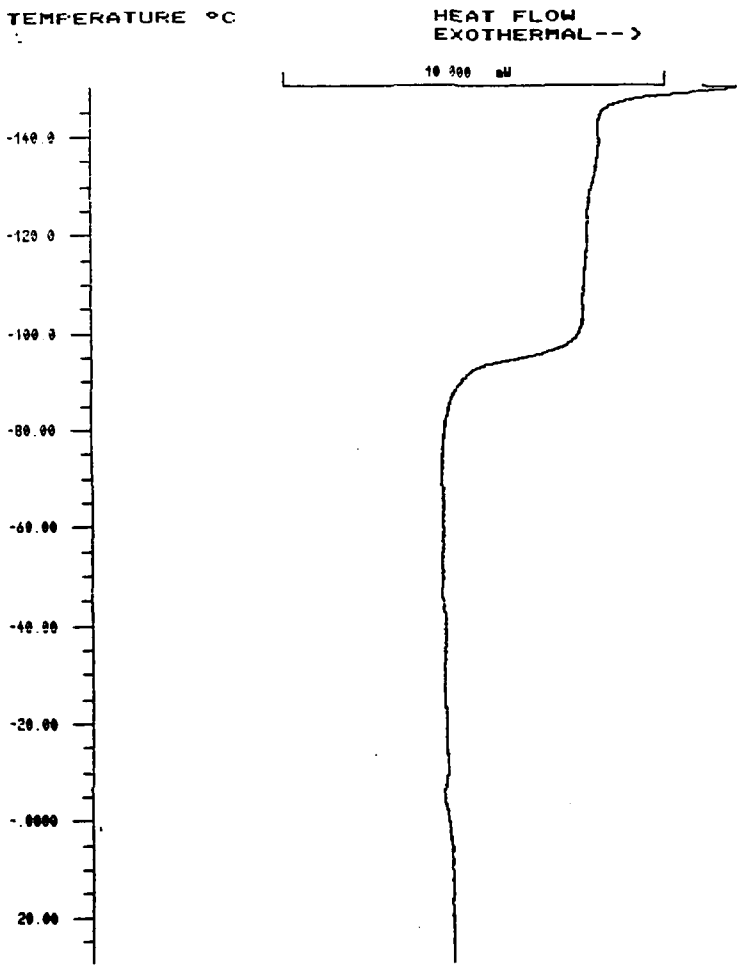

Figure 1. DSC Record of 14 Molar HAN; Heating Rate = 5°C/min

typical of molten salts.[16-19] The low temperature transition continues to appear at HAN concentrations below 11 M, although it now is not the only event observed. The magnitude of the transition decreases until it becomes undetectable at 0.4 M HAN. Table 3 presents the glass transition data.

TABLE 3. Glass Transition Data for HAN - Water Mixtures

HAN Concentration	Glass Transition		ΔC_p
mole/liter	Onset (°C)	Complete (°C)	cal/g-K
15.8	-90.15	-84.59	0.264
14.0	-98.33	-92.55	0.301
12.0	-105.25	-99.19	0.399
11.0	-108.73	-102.31	0.364
10.0	-111.50	-105.10	0.416
9.0	-114.12	-107.85	0.414
8.0	-101.79	-96.25	0.215
4.0	-102.84	-96.65	0.123
2.0	-103.47	-101.25	0.025
0.8	-105.52	-95.03	0.058
0.4	none seen		-----

Although the data show that onset and completion temperatures decrease with decreasing HAN concentration until 9 M, no firm comment can be made for samples lower in concentration than 11 M because other thermal events are also seen, creating the possibility that concentration of the samples at the time that the transition is seen is different from that of the original sample; above 11 M this is not the case. The very low temperatures obtained for glass formation are somewhat surprising but are not so unusual as to warrant special comment.

At the other concentration extreme (< 0.8 M), a large endotherm appears and Figure 2 illustrates such an observation. Although a very small glass transition was obtained with 0.8 M HAN samples, it would not be observable in Figure 2 because of the instrument span sensitivity required to display the endotherm.

The endotherm is believed to indicate sample freezing and the temperature of the endotherm peaks correspond well with calculated freezing point depressions of 1:1 electrolytes.[20]

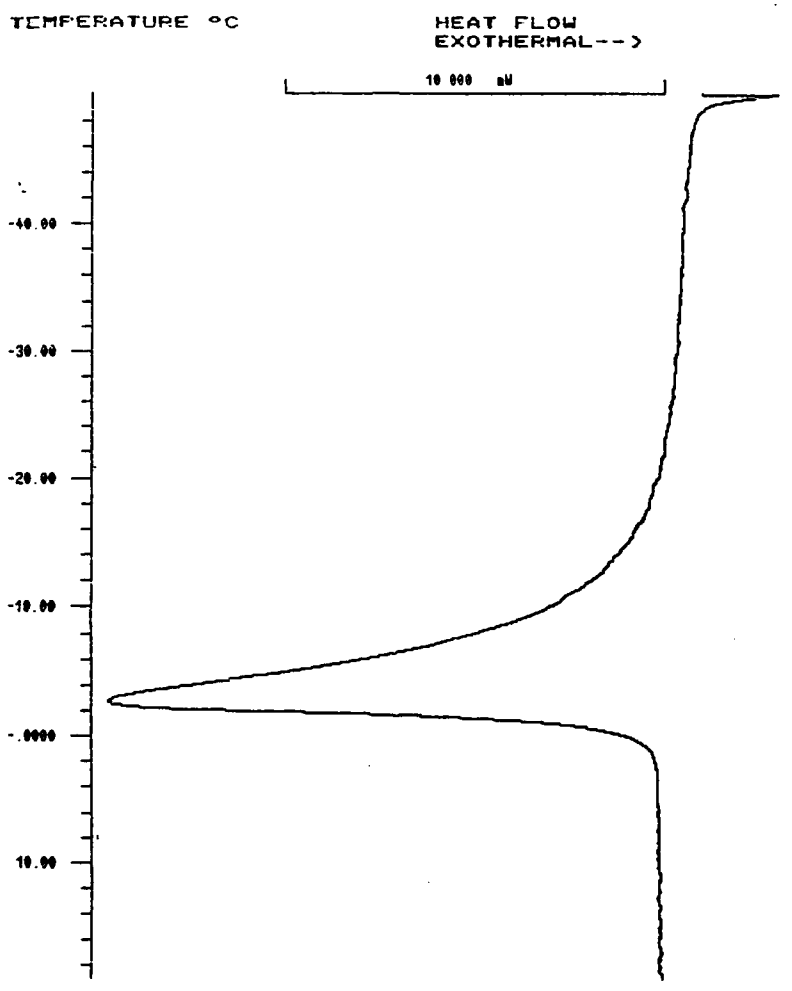

Figure 2. DSC Record of 0.8 Molar HAN; Heating Rate = 5°C/min

Between the concentration extremes, the HAN-water DSC traces become more complex, Figure 3 being an example of the complexity observed. Figure 3 is a

record, at a heating rate of 5°C/min, of 10 M HAN. A phase transition appears at -107° and a pattern of exo and endotherms are seen starting at -80°. The sample is partially solid above -100°, in contrast to the Figure 1 data. Figure 4 shows the effect of heating rate on the 10 M HAN sample. Although low temperature glass transitions are still observed, larger thermal events are seen at higher temperatures and it would appear that the glass transitions now involve only a portion of the material.

The data indicate that HAN-water mixtures have the properties of dilute aqueous solutions at low HAN concentrations and the properties of molten salts at high HAN concentrations. No attempt will be made to speculate about the composition of these molten salts at this time. At intermediate HAN concentrations the properties of both systems are seen, indicating that a gradual transition from aqueous solution to molten salt is taking place. The properties of these mixtures at intermediate concentrations are difficult to address, in part because salt and solvent concentrations in the solid and liquid phases are probably different and are also different from those of the original solutions. Isolation and analysis of the components of these heterogeneous mixtures would be difficult and probably of limited value since their composition would be dependent on both time and the specific conditions of sample size and heating or cooling rate employed. A complete phase diagram of the HAN-water system is required in order to describe the nature and composition of these mixtures properly.

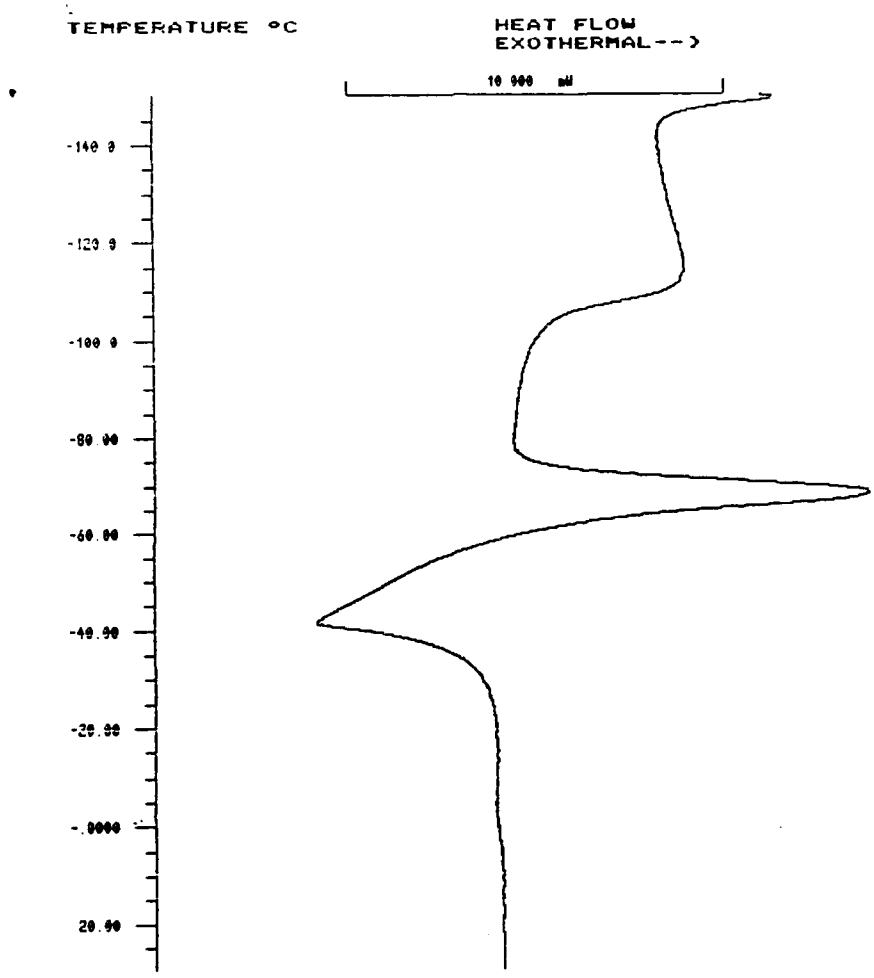

Figure 3. DSC Record of 10 Molar HAN; Heating Rate = 5°C/min

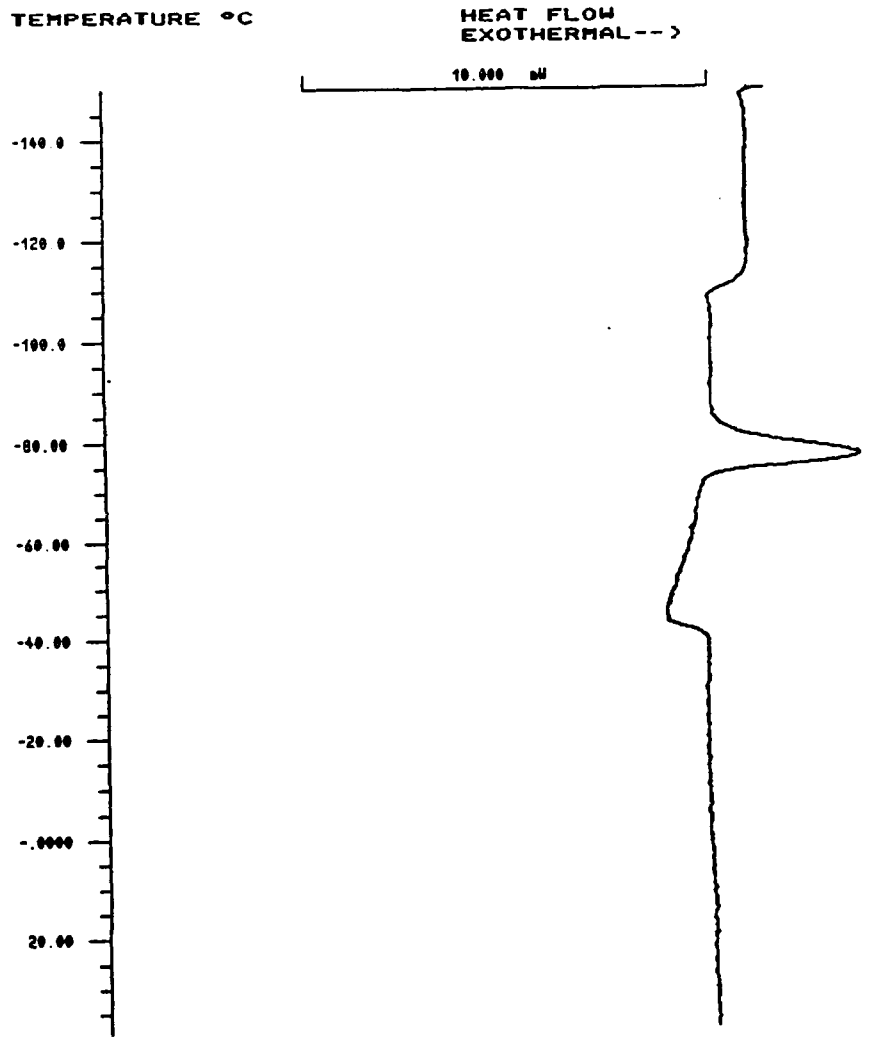

Figure 4. DSC Record of 10 Molar HAN; Heating Rate = 1°C/min

TEAN-water mixtures were studied in much the same way as were the HAN mixtures. A DSC record of 2 M TEAN is shown in Figure 5.

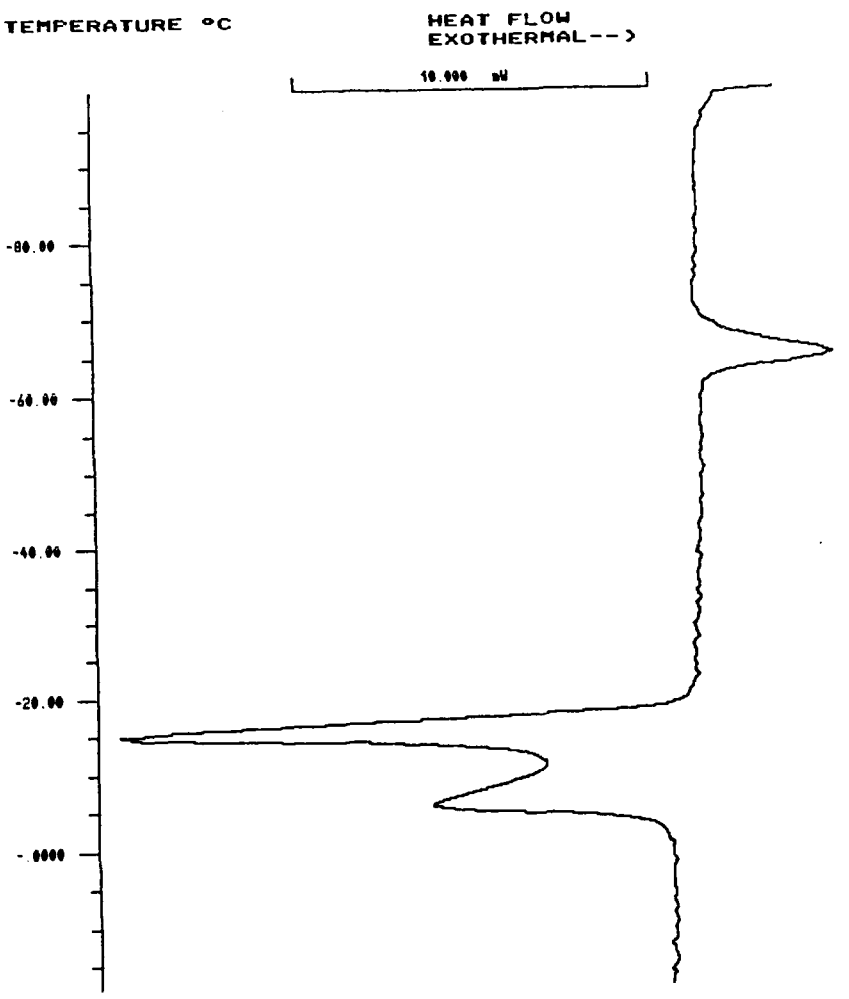

Figure 5. DSC Record of 2 Molar TEAN; Heating Rate = 5°C/min

An exotherm is seen at about -70°C and multiple endotherms are seen starting at -20°C. The temperatures at which these features appear are dependent both on TEAN concentration and on heating rate. The relative peak heights of the endotherms are strongly concentration dependent, the higher temperature peak increasing in magnitude relative to the lower temperature one as TEAN concentration decreases. The data suggest that more than one crystal form of the

salt is obtained. Possibly these crystal forms differ in the number of their waters of hydration since the relative peak heights of the endotherms observed vary with TEAN concentration. This is a logical assumption, considering the molecular structure of the salt, which contains a tertiary ammonium ion with three terminal hydroxyl groups. Hydrogen bonding between the cations and water is a distinct possibility; to a much lesser extent, so is the possibility of cation-anion bonding. This latter type of bonding, commonly called ion-pairing, has been observed in a number of ionic systems but is rarely seen at concentrations as low as the TEAN concentrations studied herein.

All of the propellants evaluated exhibited a glass transition, the only thermal event observed between -150 and 20°C. A DSC record obtained with LGP 1845 is shown in Figure 6 as a typical example. The record bears a strong resemblance to the data from 14 M HAN shown in Figure 1. Onset of a transition occurs at -89°C; the change in heat capacity associated with this transition is 0.253 cal/g-K. LGP 1846 data are quite similar, the only significant difference being that onset of the transition is seen at -102°C and the change in heat capacity is 0.279 cal/g-K. Thus the propellants LGP 1845 and 1846 exhibit calorimetric properties characteristic of low-temperature molten salt systems and do not retain the low-temperature properties of their components. Glass transitions from homogeneous liquids to homogeneous glasses are the only thermal events observed; there is no indication of component separation. The temperature at which these glass transitions occur (-89 and -102°C respectively) are sufficiently below low-

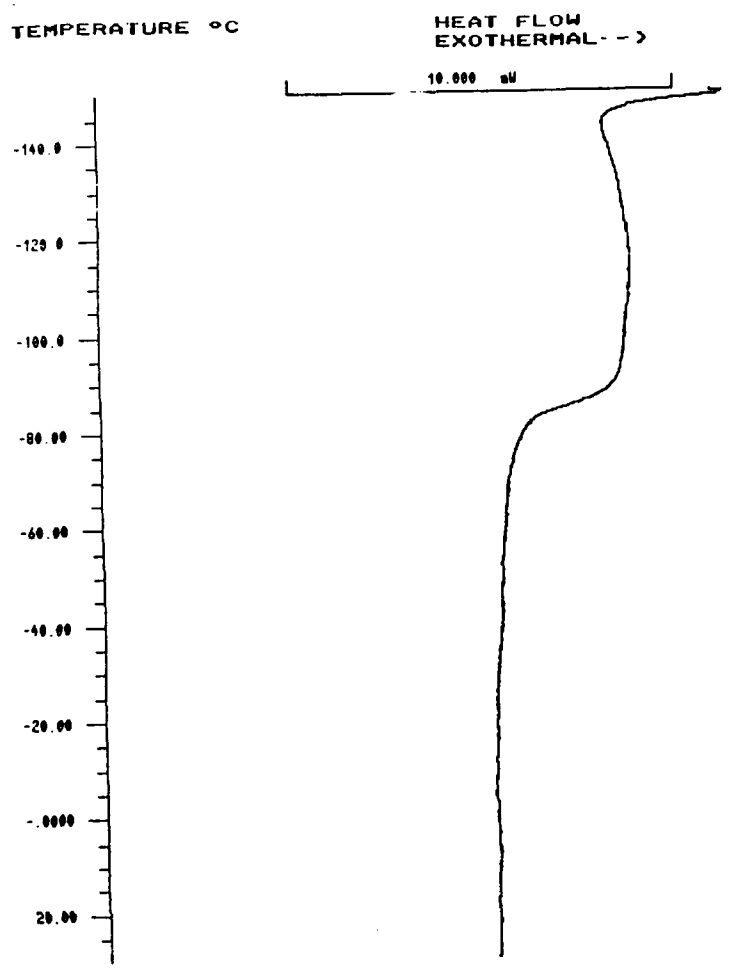

Figure 6. DSC Record of LGP 1845; Heating Rate = 5°C/min

temperature requirements for gun propellants for Army use that neither operational nor storage problems are anticipated. Note that the heat capacity of the propellant appears to be independent of temperature over its liquidus range up to 20°C, the highest temperature investigated in these studies. Note also that the phase transition in LGP 1846 is seen at a temperature 13° lower than that in LGP 1845, which illustrates the complexity of these systems,

recalling that the only difference between these mixtures is the greater water content (3.2%) of LGP 1846.

The values for the change in heat capacity associated with the glass transition for propellants 0, 1, 2, and 3 are 498, 345, 287, and 257 mcal/g-K, respectively, the heat capacity values decreasing with increasing numbers of hydroxyl groups in the AAN. The heat capacity values associated with the glass transitions are quite small for all of these propellants, indicating that the change from glass to liquid does not involve extensive changes in the molecular organization of the mixture. The trend seen with propellants 0, 1, 2, and 3 indicates that the structure of the AAN plays a role in the energy required to transit from the glass to the liquid. The presence of hydroxyl groups generally promotes hydrogen-bonding and increases the structure of the molecular aggregate. Thus, it is believed that propellant 3 is the most extensively structured. Since less energy is required to transit from the glass to the liquid we conclude that liquid propellant 3 more closely resembles the glass. This resemblance decreases sequentially as hydroxyl groups are removed from the AAN component.

2. DENSITY

Densities of all of the propellants are very well approximated by straight lines over the temperature range -10 to 65°C, the equation being

$$\rho = -mt + b$$

with ρ in g/ml and t in degrees C. Values for slope and intercept are given in Table 4.

TABLE 4. Constants for Propellant Density Equation

Propellant	Slope(m)	Intercept(b)
1845	7.1188X10-4	1.4695
1846	7.1327X10-4	1.4478
0	7.2825X10-4	1.4199
1	7.0875X10-4	1.4368
2	7.0225X10-4	1.4528
3	6.9750X10-4	1.4722

The density of LGP 1845 is higher than that of LGP 1846 at all temperatures, an expected result because the salt content of LGP 1845 is higher. In the case of propellants 0-3, where salt content is the same (11 M), density increases with increasing numbers of hydroxyl groups. An increase in the number of hydroxyl groups in the AAN, in addition to increasing the size of the molecular aggregate, as deduced from the low temperature data, also causes the aggregate to be drawn together more tightly, thus increasing density. If it is assumed that the densities of the glasses are close to the same value, then the low temperature and density data reinforce a model of the molecular structure of the mixtures.

The density of HAN solutions at concentrations between 8 and 15 Molar, a range of practical importance in propellant production, is given by the equation

$$\rho = 1.12292 + 0.03099M$$

where M is molarity. This equation is good to about 1% and is the consolidation of numerous measurements. It obviously does not give the correct density of HAN at zero molarity, because the constant was adjusted to give the best fit over the concentration range, and was not forced to fit pure water.

3. EQUATION OF STATE

Murad[21] has obtained an equation of state for concentrated salt solutions by an application of the law of corresponding states to the Tait equation of state for water. This equation fits available data for various salts. Making use of the limited data available for the bulk modulus of some liquid propellants, he obtained the following results:

$$\rho^* = \frac{1 - T^*}{1 - 0.145(1 + 5.7889\Delta t^*) \ln [(0.2165 + p^*)/0.2165]}$$

where $\rho^* = \rho \times \alpha^3$ (ρ = density, g/ml)

$$T^* = T/\beta \quad (T = \text{temperature, K})$$

$$p^* = p\alpha^3/\beta \quad (p = \text{pressure, MPa}),$$

$$\Delta t^* = (T-298.15)/\beta$$

and the constants are:

LGP	Equation of State		Surface Tension		Viscosity	
	α	β	α	β	α	β
1845	0.843912	2337	3.2927	1129	1.8141	1.1684
1846	0.847544	2303	3.1973	1039	1.7244	1.1684

Frankel and Doxbeck[10] measured sound velocity by acoustic interferometry in a solution of composition 62.3 % HAN, 19.6 % TEAN, and 18.1 % water and used the data to obtain a number of thermodynamic values. The mixture used is neither LGP 1845 nor 1846. The HAN:TEAN ratio is 3.17, the same as in the propellants, and water content is essentially midway between LGP 1845 and 1846. Their results are summarized as follows:

$$v(t) = 1966 - 1.703\ t$$

where v(t) is sound velocity at ambient pressure (m/s), and t is temperature (^{o}C),

$$K_T(t) = 1.954 \times 10^{-6} + 5.200 \times 10^{-9}\ t$$

where $K_T(t)$ is isothermal compressibility (1/MPa),

$$v(p) = 1942.79 - 15.4\ p - 6.482 \times 10^{-4}\ p^2 - 1.638 \times 10^{-7}\ p^3$$

where v(p) is sound velocity at ambient temperature, and p is pressure (MPa),

$$\rho(p) = 1.4532 + 2.9387 \times 10^{-4}\, p - 2.1711 \times 10^{-7}\, p^2 - 1.2192 \times 10^{-10}\, p^3$$

where $\rho(p)$ is density at ambient temperature (g/ml),

$$C_p = 2.29 + 9.78 \times 10^{-5}\, p$$

where C_p is heat capacity at constant pressure (J/g-K),

$$\beta(p) = 4.898 \times 10^{-4} + 5.20 \times 10^{-7}\, p$$

where $\beta(p)$ is isothermal bulk modulus at ambient temperature, and

$$K_t(p) = 2.02 \times 10^{-6} - 3.38 \times 10^{-9}\, p + 3.36 \times 10^{-12}\, p^2$$

where $K_t(p)$ is isothermal compressibility at ambient temperature.

These data were then used to obtain improved values for α and β in Murad's equation of state by a brute-force method. The two constants were adjusted until the average deviations of $\rho_{(calc)} - \rho_{(meas)}$ and $K_{(calc)} - K_{(meas)}$ both reached minima. The constants obtained in this way depended on the range and spacing of pressure values used in the computations; for the range 0-400 MPa at 1 MPa intervals, the best values were found to be α = 0.84078 and β = 2203.94. Using these values, Murad's equations reproduce experimentally determined density and isothermal compressibility as functions of pressure with zero mean deviation.

4. SURFACE TENSION

The measured values[15] for surface tension, γ, of the propellants in equilibrium with water vapor and of pure water are given in Table 5.

TABLE 5. Surface Tension as a Function of Temperature

Temp °C	Surface Tension dyne/cm		
	LGP 1845	LGP 1846	Water
-55	80.000	76.250	----
-50	79.393	75.525	----
-35	78.126	73.605	----
-15	75.590	72.219	----
0	----	----	75.584
5	73.918	70.024	75.231
10	----	----	74.755
15	----	----	73.265
25	71.618	66.901	72.102
40	----	----	70.246
45	69.789	64.556	----
50	----	----	68.195
60	----	----	66.627
65	67.163	63.243	----
70	----	----	63.789

One notes that the surface tension of LGP 1845 is consistently higher than that of 1846 and that the values for either propellant are not substantially different from those of water.

Murad has shown[21] that these results are well represented by the equation

$$\gamma^* = (1 - T^*)^{11/9},$$

where

$$\gamma^* = \gamma \alpha^2/\beta,$$

and α and β are the same constants used in the equation of state above.

The parachor[22] is defined by the equation

$$[P] = (M \times \gamma^{0.25})/(\rho_{(liq)} - \rho_{(vap)})$$

where M is the molecular weight of the substance. In the case of a single compound such as water, M is simply 18. In the case of a mixture, M is a weighted average based on composition and is 59.32 for LGP 1845 and 54.49 for LGP 1846. As discussed in the reference, [P] is almost independent of temperature. It has recently been shown[21] that this temperature independence follows from the principle of corresponding states. For non-associated liquids, parachor values are essentially additive.

At one time, the parachor was one of several additive functions that were used to explore molecular structure, but the progress of molecular structure theory and of diffraction methods have deprived it of most of its applications. Nevertheless, it is interesting to consider the data of Table 6, which shows that the parachor for LGP 1845, 1846, and for water vary only about 2% over a temperature range in which the surface tension itself varies some 18%.

TABLE 6. The Parachor of LGP 1845, 1846, and Water

Temp °C	ρ g/ml	γ dyne/cm	[P]	[P](t)/[P](r)*	γ(t)/γ(r)
			LGP 1845		
65	1.4234	67.163	119.32	1.005	0.909
45	1.4372	69.789	119.31	1.005	0.944
25	1.4517	71.618	118.88	1.002	0.969
5	1.4657	73.918	118.68	1.000	1.000
-15	1.4802	75.590	118.17	0.996	1.023
-35	1.4944	78.126	118.02	0.994	1.057
-55	1.5086	80.000	117.61	0.991	1.082
			LGP 1846		
65	1.4015	63.243	109.65	1.005	0.903
45	1.4156	64.556	109.12	1.000	0.922
25	1.4300	66.901	108.98	0.999	0.955
5	1.4445	70.024	109.13	1.000	1.000
-15	1.4585	72.219	108.92	0.998	1.031
-35	1.4728	73.605	108.38	0.993	1.051
-55	1.4870	76.250	108.29	0.992	1.089
			WATER		
70	0.9778	63.789	52.02	0.989	0.885
60	0.9832	66.627	52.31	0.994	0.924
50	0.9881	68.195	52.34	0.995	0.946
40	0.9922	70.246	52.52	0.998	0.974
25	0.9971	72.102	52.61	1.000	1.000
15	0.9991	73.265	52.70	1.002	1.016
10	0.9997	74.755	52.94	1.006	1.037
5	1.0000	75.231	53.01	1.008	1.043
0	0.9999	75.584	53.08	1.009	1.048

* [P](t)/[P](r) is the value at a given temperature divided by the value at a reference temperature and applies to both parachor and surface tension.

5. VAPOR PRESSURE

The measured vapor pressures of propellants LGP 1845 and 1846 are presented in Table 7.

TABLE 7. Vapor Pressure Data for LGP 1845 and 1846

Temp °C	Vapor Pressure (mm)		Temp °C	Vapor Pressure (mm)	
	1845	1846		1845	1846
-5	1.68	1.95	25	10.2	11.5
0	2.50	2.65	35	18.2	20.2
5	3.42	4.02	45	31.2	34.8
10	4.72	5.28	55	51.5	57.0
15	6.40	7.08	65	81.8	89.2

The change in vapor pressure with temperature of a liquid at equilibrium is given by the Clapeyron-Clausius equation[23]

$$d(\ln P)/d(1/T) = \Delta H_v/R$$

where P is pressure (mm), T is temperature (K), ΔH_v is latent heat of vaporization (cal/mole), and R is the universal gas constant (1.987 cal/mole-K).

Values of ΔH_v for water, LGP 1845, and 1846 derived from the data are 579.0, 546.8, and 542.3 cal/g. The small temperature range and experimental noise of the data do not permit a meaningful estimate of the temperature dependence of the heats of vaporization to be made.

One can extrapolate the data and obtain the temperature below which the vapor pressure of the propellants should be higher than that of the pure water component. These temperatures are -11.6 and -4.5 °C for LGP 1845 and 1846, respectively. The probable significance of these results are that since both

extrapolated values are lower than the water freezing point, the data indicate that the vapor pressures of the propellants are lower than the vapor pressure of their water components over their entire liquidus range.

The vapor pressure data were fitted to a 3-constant equation. Table 8 gives a comparison of the fitted vapor pressures of water, LGP 1845, and LGP 1846.

TABLE 8. Comparison of the Fitted Vapor Pressures of Water and the Two Liquid Propellants

Temp °C	Vapor Pressure mm			Ratios		
	Water	1845	1846	1845/Water	1846/Water	1846/1845
-5.0	3.16	1.8	2.0	0.56	0.63	1.13
0.0	4.58	2.4	2.8	0.53	0.60	1.13
5.0	6.54	3.4	3.8	0.51	0.58	1.13
10.0	9.20	4.6	5.1	0.49	0.56	1.12
15.0	12.78	6.1	6.9	0.48	0.54	1.12
25.0	23.75	10.9	12.1	0.46	0.51	1.12
35.0	42.17	18.7	20.8	0.44	0.49	1.11
45.0	71.89	31.2	34.6	0.43	0.48	1.11
55.0	118.10	50.9	56.2	0.43	0.48	1.10
65.0	187.62	81.2	89.1	0.43	0.47	1.10

The vapor pressure of LGP 1846 is approximately 11% higher than that of LGP 1845, a ratio that is almost independent of temperature. This number can be interpreted in view of the fact that the water content of LGP 1846 is 11% higher than that of LGP 1845. The ΔH_v values for LGP 1845 and 1846 are about 6% lower than the corresponding value for water, an indication of the effect of hydrogen-bonding by the salts. The salt-water hydrogen bonds are stronger than the bonds formed by the solvent with itself, indicating the formation of

a rather well organized and extensive molecular network in the propellant. The correlation of increased vapor pressure with increased water content indicates that this molecular network is fully formed in LGP 1845 so that a small increase in water content simply places the additional water in space external to the network.

Additional information regarding the nature of such interactions cannot be inferred from these data. As is characteristic of solutions of ionic salts, the vapor pressure of the propellants is due exclusively to the water present; the physical and chemical properties of the propellant vapor are those of water vapor.

The fitted vapor pressures for LGP 1845 and 1846 can be extrapolated to calculate an estimated boiling point for the propellants. The data in Table 5 produce boiling points of 126.5 and 123.7 ^{o}C for LGP 1845 and 1846, respectively. These values cannot be reliably measured because initiation of thermal decomposition of either HAN or of propellant mixtures such as LGP 1845 or 1846 takes place at temperatures near the calculated boiling points.[5] These extrapolated boiling points indicate that a thermal reaction initiation mechanism probably does not require or involve significant removal of water from the mixtures. This point had been made previously[24] and was supported by a body of data separate from that presented here. It is satisfying to be able to present an independent argument in support of the same conclusion.

6. VISCOSITY

Viscosity, electrical conductivity, thermal conductivity, and diffusion are closely related at the molecular level,[25] so it is appropriate to discuss them together; unfortunately, data are available only for the first two.

It has been known for some time[16-18 26] that the temperature dependence of diffusion, electrical conductivity, and viscosity can all be well represented by the Vogel-Tammann-Fulcher (VTF) equation,

$$W(T) = AT^{-1/2}\exp[-B/(T - T_o)]$$

where W(T) is either diffusion constant, D, specific resistance, κ, or dynamic viscosity, μ. Our numerical work indicated that the $T^{-1/2}$ term in this equation was insignificant, and does not appear subsequently. Angell[27-28] had made the same simplification.

The value of T_o in the VTF equation is related to, but somewhat lower than the glass transition temperature, T_g.[18] The values of T_o used in the VTF equation are usually obtained by curve fitting the experimental data.

Kinematic viscosity data obtained as a function of temperature with propellants 0, 1, 2, and 3 are presented in Table 9.

TABLE 9. Kinematic Viscosity Data

Temp °C	Kinematic Viscosity (cSt)			
	3	2	1	0
65	2.62	2.29	2.25	2.12
45	3.82	3.34	3.24	3.00
25	6.38	5.47	5.24	4.74
5	12.63	10.78	10.20	8.88
-15	35.56	27.87	25.64	21.49
-35	185.68	134.58	118.56	90.35
-45	624.77	429.12	367.58	258.93
-55	3233.89	2020.94	1716.25	1083.35

Table 9 shows that kinematic viscosity increases with decreasing temperature and with the number of hydroxyl groups in the AAN. The data in Table 9 show that LGP 1845 is the most viscous propellant of its general type. However, the range of values obtained for propellant 3 is comparable to those of hydraulic fluids certified for use at low temperature[6] and therefore ought not to pose major problems for gun system designers.

The effect of decreasing temperature and the presence of hydroxyl groups in the AAN on the density of the propellants have already been discussed; both variables contribute to an increase in density. Since dynamic viscosity is the product of kinematic viscosity and density, the effects seen in Table 9 will be enhanced when dynamic viscosity is considered. Dynamic viscosity values as a function of temperature are presented in Table 10.

TABLE 10. Dynamic Viscosities of Four Propellants

Temperature °C	Temperature K	Dynamic Viscosity (cP) 3	2	1	0
65	338	3.74	3.22	3.13	2.91
45	318	5.50	4.75	4.55	4.16
25	298	9.28	7.85	7.44	6.64
5	278	18.6	15.6	14.6	12.6
-15	258	52.7	40.8	37.1	30.8
-35	238	278.	199.	173.	131.
-45	228	939.	637.	540.	376.
-55	218	4885.	3014.	2533.	1582.

A "best" value of T_o was obtained for each of these systems in the following way. The linear-least-squares formalism was applied to the equation

$$\ln\mu = A + [B/(T - T_o)]$$

for a range of T_o values. The mean-square relative error, S, for N points, defined as

$$S^2 = \Sigma\{100[(\mu_{exp}-\mu_{calc})/\mu_{exp}]^2\}/(N-1),$$

was computed for a range of T_o values; the T_o that minimized S was arbitrarily chosen as the "best" value. (Note that S was computed using μ directly, not $\ln\mu$). A change of $\pm$ 5 K in T_o changed S by about a factor of 3. This numerical procedure can find T_o with great precision. The value obtained for T_o by this method is to be compared with T_g, an experimentally determined quantity that is probably no better than $\pm$ 5 K.

The dynamic viscosity data for the four propellant mixtures taken in accordance with the VTF equation produce the residual errors plotted in Figure 7.

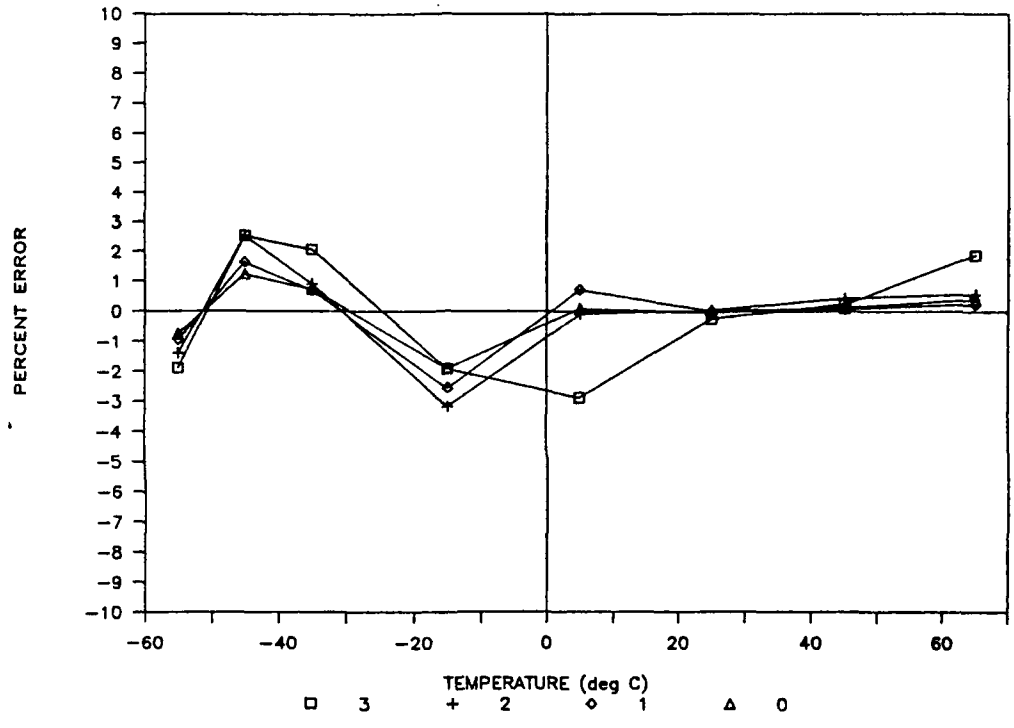

Figure 7. Percent Deviation From Linearity of the VTF Fittings

The values of T_o, obtained from the regression analysis, and T_g obtained from the low temperature studies, are included in Table 11.

TABLE 11. Values of the Constants in the VTF Equation for Viscosity of the Propellants

Propellant	T_o (K)	B (cal/g)	S (%)	T_g (K)
3	167.6	518.2	2.1	172.5
2	166.6	505.6	1.7	175.0
1	167.4	484.4	1.3	173.2
0	166.0	472.0	0.96	171.8
LP 1845	165.4	526.2	2.0	
LP 1846	164.7	494.1	1.6	

On average, T_o is 6 degrees lower than T_g. An accurate value of T_g is obtained with great difficulty for a number of reasons. The values of T_g cited throughout this report are the onset temperatures of the transition; although the selection is consistent, it is not necessarily the best choice. Furthermore, glass transition temperatures are known to be affected by supercooling, sample size, the nature of the surface on which the samples are placed, the shape of the samples, etc. The 6 degree difference between T_g and T_o obtained supports published arguments that indicate that, although viscosity is strongly affected by the structure of the AAN salt (producing viscosity values that differ by as much as 3300 cP at -55°C), the difference in T_g-T_o is maintained.

Murad[21] has shown that the effect of pressure on the viscosity of these propellants is given to about 2% by

$$\ln(\mu^*) = - 9.3737 + 2907.9\ \rho^*/(T^* - 141.25)$$

where M is the mean molecular weight of the mixture,

$\mu^* = \mu\ \alpha/(M\beta)^{1/2}$, the other terms having been previously described.

7. ELECTRICAL CONDUCTIVITY

A precise definition of conductivity (often called specific conductance) is given in many places; e.g.[29 30] The unit of conductivity, $1/\kappa$, to be used is the Siemen per centimeter (S/cm); the Siemen was commonly called the reciprocal ohm or mho.

The conductance of ionic liquids depends on temperature and concentration. The conductivity of LGP 1845, 1846 and of 11 M HAN as a function of temperature has recently been measured by Vanderhoff and coworkers in a set of careful experiments.[31] Their data are reproduced in Tables 12, 13, and 14.

TABLE 12. Specific Conductance of LGP 1845 as a Function of Temperature

Temp °C	$1/\kappa$ (S/cm)	Temp °C	$1/\kappa$ (S/cm)	Temp °C	$1/\kappa$ (S/cm)
-47.0	0.000820	-11.4	0.0190	17.1	0.0596
-44.9	0.000954	-10.0	0.0206	18.3	0.0616
-42.5	0.00142	-8.3	0.0223	19.4	0.0637
-40.9	0.00173	-7.0	0.0238	20.5	0.0655
-38.6	0.00216	-5.9	0.0250	23.9	0.0746
-35.9	0.00298	-4.7	0.0264	31.8	0.0906
-34.2	0.00353	-3.7	0.0277	34.6	0.0963
-30.3	0.00503	-2.5	0.0291	36.5	0.100
-28.7	0.00576	-0.8	0.0314	37.6	0.103
-26.9	0.00667	0.9	0.0340	39.2	0.107
-25.5	0.00741	2.7	0.0362	41.0	0.111
-23.7	0.00869	4.1	0.0382	43.0	0.115
-22.8	0.00929	5.2	0.0398	44.6	0.119

TABLE 12. Specific Conductance of LGP 1845 as a Function of Temperature (Con't)

Temp °C	1/κ (S/cm)	Temp °C	1/κ (S/cm)	Temp °C	1/κ (S/cm)
-21.8	0.00997	6.3	0.0415	45.0	0.120
-21.2	0.0104	7.6	0.0433	46.2	0.122
-20.7	0.0108	8.8	0.0456	47.9	0.126
-20.1	0.0113	10.2	0.0477	49.7	0.130
-19.5	0.0117	11.5	0.0498	51.8	0.135
-18.6	0.0124	12.7	0.0517	54.3	0.141
-17.8	0.0131	13.8	0.0537	55.6	0.144
-14.8	0.0157	14.9	0.0557	56.8	0.147
-14.0	0.0164	15.9	0.0575	59.4	0.153
-12.8	0.0177				

TABLE 13. Specific Conductance of LGP 1846 as a Function of Temperature

Temp °C	1/κ (S/cm)	Temp °C	1/κ (S/cm)	Temp °C	1/κ (S/cm)
-60.1	0.000196	-13.1	0.0231	30.6	0.0979
-57.9	0.000272	-10.3	0.0264	32.8	0.103
-55.6	0.000352	-7.0	0.0308	35.2	0.108
-52.9	0.000527	-3.8	0.0346	36.9	0.112
-50.2	0.000830	-0.6	0.0394	39.0	0.117
-47.7	0.00117	2.7	0.0445	40.9	0.122
-44.5	0.00181	5.9	0.0495	42.6	0.125
-41.1	0.00267	8.3	0.0537	44.5	0.129
-38.6	0.00422	10.7	0.0603	46.7	0.136
-36.1	0.00514	12.9	0.0619	48.9	0.140
-33.2	0.00632	15.1	0.0659	51.1	0.146
-29.9	0.00819	17.4	0.0707	53.4	0.151
-27.2	0.00994	19.5	0.0747	55.6	0.157
-24.7	0.0118	21.8	0.0797	57.8	0.165
-22.1	0.0140	24.1	0.0844	60.0	0.171
-19.1	0.0167	26.2	0.0894	62.2	0.177
-15.8	0.0203	28.4	0.0941		

TABLE 14. Specific Conductance of 11 Molar HAN as a Function of Temperature

Temp °C	1/κ (S/cm)	Temp °C	1/κ (S/cm)	Temp °C	1/κ (S/cm)
-59.9	0.00090	-14.6	0.0438	26.4	0.161
-59.0	0.00103	-13.0	0.0462	27.8	0.165
-57.9	0.00126	-10.0	0.0526	30.7	0.175
-54.4	0.00191	-7.3	0.0586	32.5	0.181
-52.9	0.00241	-4.1	0.0658	33.8	0.185
-51.0	0.00291	-0.6	0.0756	35.2	0.189

TABLE 14. Specific Conductance of 11 Molar HAN as a Function of Temperature (Con't)

Temp °C	1/κ (S/cm)	Temp °C	1/κ (S/cm)	Temp °C	1/κ (S/cm)
-49.2	0.00336	3.6	0.0848	36.9	0.195
-46.6	0.00451	4.9	0.0883	39.2	0.203
-43.3	0.00627	13.8	0.119	41.6	0.209
-40.7	0.00807	16.6	0.128	43.5	0.216
-37.7	0.0105	18.0	0.132	46.0	0.225
-34.2	0.0138	20.6	0.140	49.0	0.235
-28.4	0.0207	21.4	0.144	53.0	0.248
-24.7	0.0262	23.2	0.150	53.8	0.250
-20.9	0.0321	24.3	0.154		
-17.3	0.0377	24.7	0.155		

The VTF equation was applied to the Table 12, 13, and 14 data and results are shown in Figures 8, 9, and 10. Generally, viscosity decreases with increasing temperature whereas conductivity increases. In order to facilitate direct comparison of Figures 8-10 with the viscosity data, specific resistance, κ^{-1} was used in plotting the data.*

---

*The VTF equation applies to equivalent conductance, Λ. For 1:1 electrolytes, Λ is κ divided by molarity, constants in the three cases addressed in Tables 12-14. Equivalent and specific conductance are related by density, a property that changes with temperature. Density data are available for LGP 1845 and 1846, but using them did not change the derived parameters.

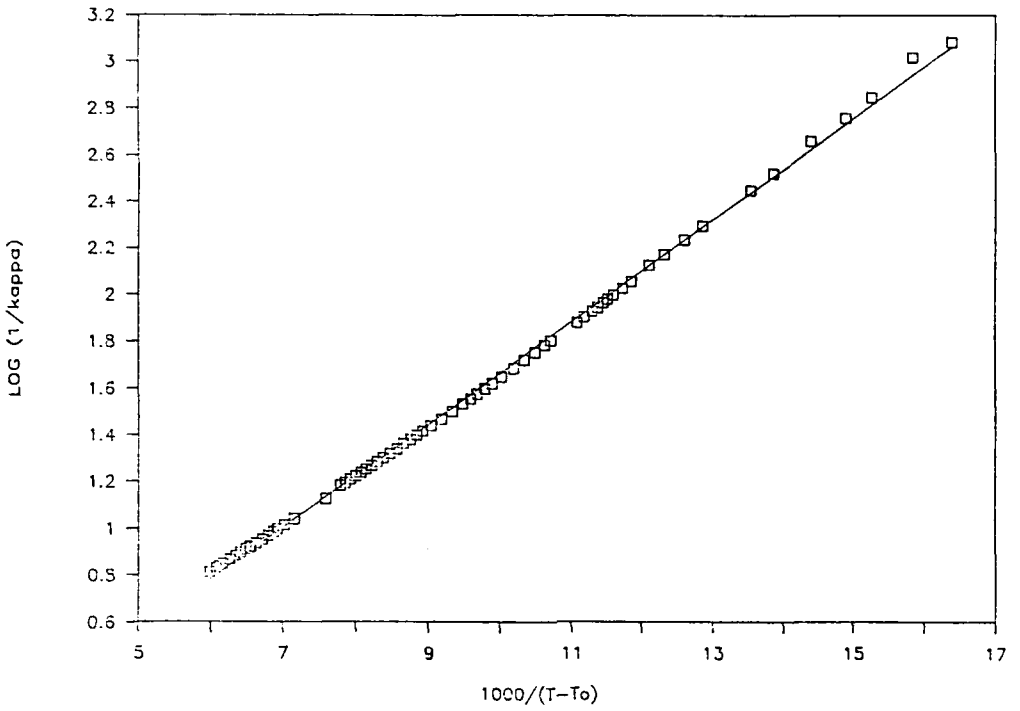

Figure 8. Application of the VTF Equation to LGP 1845 Conductance Data

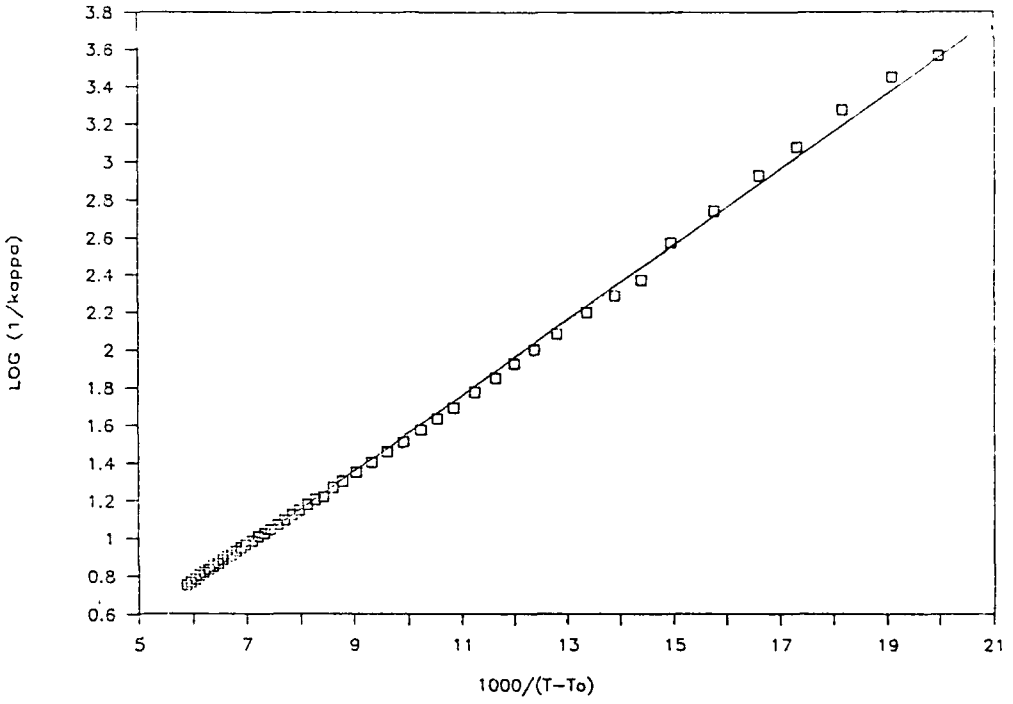

Figure 9. Application of the VTF Equation to LGP 1846 Conductance Data

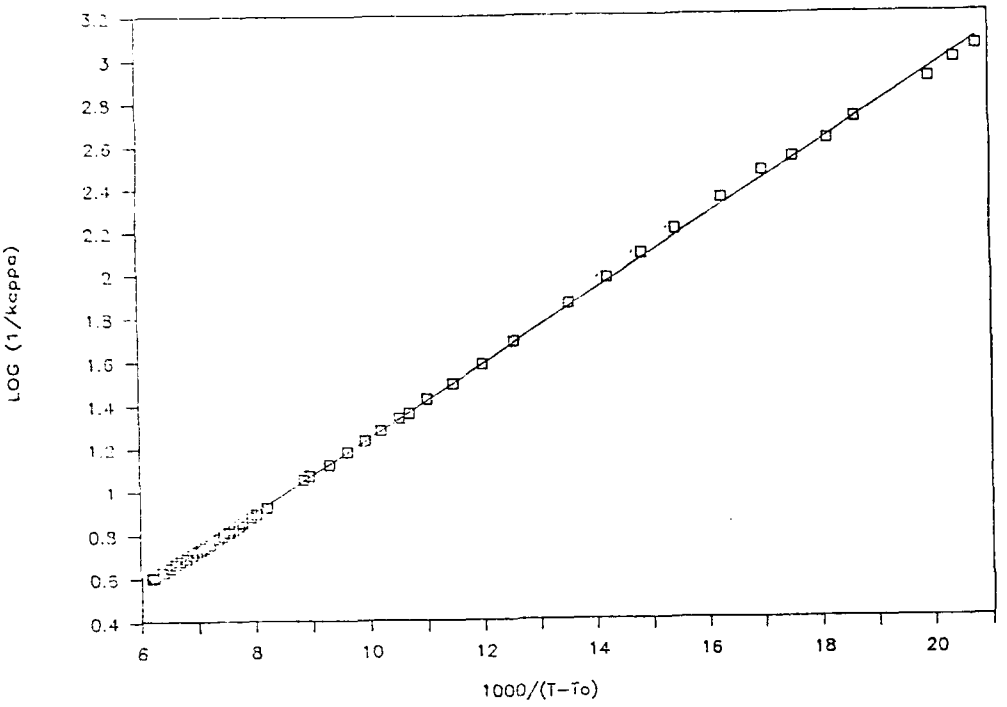

Figure 10. Application of the VTF Equation to 11 M HAN Conductance Data

Values of the VTF equation parameters obtained are given in Table 15.

TABLE 15. Values of the Constants in the VTF Equation From Conductivity Data

Sample	T_o (K)	B (cal/g)	S (%)
LGP 1845	174.1	413.7	2.1
LGP 1846	170.4	404.0	2.0
11 M HAN	162.1	423.6	3.4

Values of T_o for the three data sets are in excellent agreement with those in Table 11, obtained using viscosity data. In all three cases, goodness of fit

of the VTF equation is excellent and provides additional support for its use in describing the transport properties of these mixtures. Values of B obtained by Moynihan[17] using conductivity data for molten $Ca(NO_3)_2$ and $Na_2S_2O_3$ ranged from 464 to 689 cal/g and compare reasonably well with values in Table 15, thus providing additional evidence that the HAN-based mixtures behave as molten salts.

Values of T_g for the samples used to obtain the data in Tables 12-14 are not available; a selection of T_g values from other, similar mixtures in order to evaluate T_g-T_o carries with it some risk. The extent of this risk is illustrated by comparison of T_g values for LGP 1845 and propellant 3, two mixtures that are, in principle, identical. The experimental values of T_g obtained for these samples are 184.2 and 172.5 K; although the 172.5 value seems more consistent with other data generally, there is no <u>a priori</u> basis for preferring it.

V. SUMMARY AND CONCLUDING REMARKS

A number of the physical properties of the HAN-based propellants LGP 1845 and 1846 and of their separate components have been measured or estimated. In addition, the effect of molecular structure of the AAN component of the propellant on physical properties has been studied. The intent of these studies was to produce a self-consistent model of the mixtures that will permit prediction of physical properties not yet measured and the effect of temperature and pressure variation on them. In general, this effort has been

successful.

The candidate gun propellants LGP 1845 and 1846 are homogeneous liquids that do not undergo any phase transitions over the entire temperature range of military interest. Their vapor pressure is less than the vapor pressure of the water that they contain; their vapors contain only water. Density and viscosity increase with decreasing temperature, density increasing linearly and viscosity varying in accordance with the VTF equation as it applies to molten salts. Although physical property variations must be incorporated into the design of liquid propellant gun components, this variation is not expected to inhibit proper gun functioning over the entire operational range of the gun.

On a molecular scale, the properties measured lead to a model of the system that is consistent with data available for related materials. HAN-water mixtures at low HAN concentration are aqueous solutions of a 1:1 electrolyte. HAN strongly encourages hydrogen-bonding both with itself and with solvent; as concentration increases, the system gradually changes from an aqueous solution to a molten salt that solidifies at temperatures well below the freezing point of either of its components. This hydrogen-bonding tendency, when combined with the rather low melting point of the pure salt, permits existence of salt-water mixtures that are homogeneous liquids at room temperature that contain over 90 weight-per cent salt. Since no phase transitions are observed for 80 wt-% mixtures over the temperature range -55 to +65^{o}C, physical properties vary smoothly and monotonically. Density shows

a simple constriction of the system with decreasing temperature; vapor pressure shows the effect of enhanced hydrogen-bonding, the pressure being consistently lower than that of the appropriate mole fraction of pure water.

TEAN-water mixtures are more complex. The molecular weight and melting point of TEAN (212 and 80.4°C) are higher than those of HAN (96 and 48°C); TEAN-water mixtures do not exhibit homogeneity over the broad concentration range observed for HAN. TEAN seems to behave much like an ordinary ionic salt, forming saturated solutions that are approximately 5 Molar at room temperature. The low temperature properties of the mixtures show the existence of what may be a number of TEAN-water molecular compounds. The formation of such compounds would not be unusual, and the stepwise formation of several hydrogen-bonded complexes is expected since three hydroxyl groups are readily available for complex formation.

A practical consequence of the TEAN-water data relates to propellant formulation. Since LGP 1845 is currently considered a Class B explosive, while its components HAN and TEAN are classified only as oxidizers, it has been suggested that the components be stored and transported separately in order to decrease vulnerability, reduce cost in shipping, and generally improve safety. Propellant would then be prepared by combining the components at or near locations where it would be used. The low temperature data indicate that while HAN-water and propellant mixtures will remain homogeneous liquids over their entire operational temperature range, TEAN-water mixtures will not: crystallization will occur at lower temperatures. Component

blending in order to formulate propellant will require a controlled temperature environment, a condition obtained only with difficulty in the field.

Mixtures of HAN, an AAN, and water at concentrations near those of the propellants have the properties of a molten salt, the AAN having been incorporated into a large matrix that suppresses the properties of the AAN. These matrices are strongly dependent on the structure of the AAN; additional hydroxyl groups extend the size and coherence of the matrix. Evidence for this is found in systematic changes of both the equilibrium and transport properties of the mixtures.

If, in fact, the propellants exist as extended matrices of HAN, TEAN, and water that are organized in a systematic way, then such structures could affect chemical reactivity and reaction rates. Molecular orientation and collision frequency determines the values of activation energy needed to initiate reactions and diffusion of reacting species in solution is often a limiting factor in establishing reaction rates. If the system is well organized to begin with, it is reasonable to expect such organization to influence initiation of reaction and reaction pathways and rates once reaction has been initiated. Although the extent of these effects cannot be assessed from available data, a basis for possibly abnormal reaction dynamics does exist and should be considered in studying ignition and combustion phenomena involving these mixtures.

REFERENCES

1. Klein, N., "Isomer Effects on Liquid Propellant Performance," Proc. 19th JANNAF Combustion Meeting, Vol I, p. 513, CPIA Pub. 366, Chemical Propulsion Information Agency, Laurel, MD (1982).

2. Klein, N., "Preparation and Characterization of Several Liquid Propellants," Rept. ARBRL-TR-02471, U.S. Army Ballistic Research Laboratory, Aberdeen Proving Ground, MD, 1983.

3. Klein, N., "Liquid Propellants for Use in Gun--A Review," Rept. BRL-TR-2641, U.S. Army Ballistic Research Laboratory, Aberdeen Proving Ground, MD, 1985.

4. Morrison, W.F., Knapton, J.D., and Klingenberg, G., "Liquid Propellants for Gun Applications," Rept. BRL-TR-2632, U.S. Army Ballistic Research Laboratory, Aberdeen Proving Ground, MD, 1985.

5. Sasse', R.A. and Klein, N., "Thermal Initiation of Hydroxylammonium Based Gun Propellants," Proc. 15th JANNAF Combustion Meeting, Vol. I, p. 313, CPIA Pub. 297, Chemical Propulsion Information Agency, Laurel, MD (1979).

6. Knapton, J. D. and Morrison, W. F., "Low Temperature Properties of HAN-Based Liquid Propellants," Rept. BRL-MR-3477, U.S. Army Ballistic Research Laboratory, Aberdeen Proving Ground, MD, 1985.

7. Decker, M. M., Freedman, E., Ward, J. R., Tarantino, P. A., and Davis, P. M., "Transition Metal Reactions in HAN-Based Monopropellants", Proc. 22nd JANNAF Combustion Meeting, Vol I, p 177, CPIA Pub. 432, Chemical Propulsion Information Agency, Laurel, MD, (1985).

8. Young, S., "The Vapor Pressures, Specific Volumes, Heats of Vaporization, and Critical Constants of Thirty Pure Substances", Sci. Proc. Royal Soc. (Dublin), Vol 2, p 374, 1910.

9. Biddle, R.A., "Concentration of HAN Solution," Contract DAAD05-84-M-6657 Final Report, Elkton Division, Morton Thiokol, Inc., Elkton, MD, 1985.

10. Frankel, J. and Doxbeck, M., "The High Pressure Sound Velocity and Equation of State of Aqueous Solutions of Hydroxylammonium Nitrate and Triethanolammonium Nitrate," J. Energetic Materials - in press.

11. Adamson, A.W., "Physical Chemistry of Surfaces," 2nd Ed. Wiley-Interscience, NY, 1967.

12. Smith, A. and Menzies, A.W.C., "A Static Method For Determining the Vapor Pressure of Solids and Liquids," J. Am. Chem. Soc. Vol 32, pp 1412-1434, 1910.

13. "The Physico-Chemical Constants of Binary Systems in Concentrated Solutions," Vol. 3, J. Timmermans, ed., Interscience Publishers, Inc., NY, p 777, 1960.

14. Partington, J.R., "An Advanced Treatise on Physical Chemistry," Vol. 2, J. Wiley and Sons, Inc., London, p 80, 1951.

15. Messina, N.A., Tseng, H.H., Ingram, L.S., and Summerfield, M., "The Role of Physical Properties in Dynamic Loading Processes and Bubble Collapse of Liquid Monopropellants for LPG Applications," Proc. 21st JANNAF Combustion Meeting, Vol II, p 515, CPIA Pub. 412, Chemical Propulsion Information Agency, Laurel, MD, (1984).

16. Angell, C.A., "Free Volume Model for Transport in Fused Salts," J. Phys. Chem. Vol 68, pp 1917-1929, 1964.

17. Moynihan, C.T., "The Temperature Dependence of Transport Properties of Ionic Liquids," J. Phys. Chem. Vol 70, pp 3399-3403, 1966.

18. Angell, C.A. and Smith, D.L., "Test of the Entropy Basis of the Vogel-Tammann-Fulcher Equation," J. Phys. Chem. Vol 86, pp 3845-3852, 1982.

19. Seward, R.P., "The Conductance and Viscosity of Highly Concentrated Aqueous Solutions of Hydrazinium Chloride and Hydrazinium Nitrate," J. Am. Chem. Soc. Vol 77, pp 905-907, 1955.

20. Moore, W. J., "Physical Chemistry," 3rd ed., Prentice Hall Inc., Englewood Cliffs, NJ, p 133, 1962.

21. Murad, S., "Interim Report on Army Research Office Short Term Analytical Study," (1986). (To be published)

22. Glasstone, S., "Textbook of Physical Chemistry," D. Van Nostrand Co., Inc., p 526, 1946.

23. ibid. p 450.

24. Klein, N., Sasse', R.A., Scott, R.L., and Travis, K.E., "Thermal Decomposition of Liquid Monopropellants," BRL Report No. 1970, US Army Ballistic Research Laboratories, Aberdeen Proving Ground, MD, 1977.

25. Hirschfelder, J.O., Curtiss, C.F., and Bird, R.B., "Molecular Theory of Gases and Liquids," John Wiley, NY, pp 624-633, 1954.

26. Smedley, S.I., "The Interpretation of Ionic Conductivity in Liquids," Plenum Press, NY, p 82, 1980.

27. Angell, C.A., "Electrical Conductance of Ionic Liquids with Water Content in the Range 0-80 Mole Percent," Aust. J. Chem. Vol 23, pp 929-937, 1970.

28. Angell, C.A. and Bressel, R.D., "Fluidity and Conductance in Aqueous Electrolyte Solutions," J. Phys. Chem. Vol 76, pp 3244-3253, 1972.

29. Smedley, S.I., ref cited, pp 2-4.

30. Adamson, A.W., "A Textbook of Physical Chemistry," Academic Press, NY, pp 486-492, 1973.

31. Vanderhoff, J.A., Bunte, S.W., and Donmeyer, P.M., "Electrical Conductance of Liquid Propellants: Theory and Results," Rept. BRL-TR-2741, U.S. Army Ballistic Research Laboratory, Aberdeen Proving Ground, MD, 1986.

DISTRIBUTION LIST

No. of Copies	Organization
12	Commander Defense Technical Info Center ATTN: DTIC-DDA Cameron Station Alexandria, VA 22304-6145
1	Director Defense Advanced Research Projects Agency ATTN: H. Fair 1400 Wilson Boulevard Arlington, VA 22209
1	HQDA DAMA-ART-M Washington, DC 20310
1	Commander US Army Materiel Command ATTN: AMCDRA-ST 5001 Eisenhower Avenue Alexandria, VA 22333-0001
13	Commander Armament R&D Center US Army AMCCOM ATTN: SMCAR-TSS SMCAR-TDC SMCAR-SCA, B. Brodman R. Yalamanchili SMCAR-AEE-B, D. Downs A. Beardell SMCAR-LCE, N. Slagg SMCAR-AEE-B, W. Quine A. Bracuti J. Lannon SMCAR-CCH, R. Price SMCAR-FSS-A, L. Frauen SMCAR-FSA-S, H. Liberman Picatinny Arsenal, NJ 07806-5000
4	Director Benet Weapons Laboratory Armament R&D Center US Army AMCCOM ATTN: SMCAR-LCB-TL E. Conroy A. Graham J. Frankel Watervliet, NY 12189
1	Commander US Army Armament, Munitions and Chemical Command ATTN: SMCAR-ESP-L Rock Island, IL 61299-7300
1	Commander US Army Aviation Research and Development Command ATTN: AMSAV-E 4300 Goodfellow Blvd St. Louis, MO 63120
1	Commander Materials Technology Lab US Army Laboratory Cmd ATTN: SLCMT-MCM-SB M. Levy Watertown, MA 02172-0001
1	Director US Army Air Mobility Rsch and Development Lab Ames Research Center Moffett Field, CA 94035
1	Commander US Army Communications Electronics Command ATTN: AMSEL-ED Fort Monmouth, NJ 07703

DISTRIBUTION LIST

No. of Copies	Organization
1	Commander ERADCOM Technical Library ATTN: STET-L Ft. Monmouth, NJ 07703-5301
1	Commander US Army Harry Diamond Labs ATTN: SLCHD-TA-L 2800 Powder Mill Rd Adelphi, MD 20783
1	Commander US Army Missile Command Rsch, Dev, & Engr Ctr ATTN: AMSMI-RD Redstone Arsenal, AL 35898
1	Commander US Army Missile & Space Intelligence Center ATTN: AIAMS-YDL Redstone Arsenal, AL 35898-5500
1	Commander US Army Belvoir R&D Ctr ATTN: STRBE-WC Tech Library (Vault) B-315 Fort Belvoir, VA 22060-5606
1	Commander US Army Tank Automotive Cmd ATTN: AMSTA-TSL Warren, MI 48397-5000
1	Commander US Army Research Office ATTN: Tech Library PO Box 12211 Research Triangle Park, NC 27709-2211
1	Director US Army TRADOC Systems Analysis Activity ATTN: ATAA-SL White Sands Missile Range NM 88002
1	Commandant US Army Infantry School ATTN: ATSH-CD-CSO-OR Fort Benning, GA 31905
1	Commander Armament Rsch & Dev Ctr US Army Armament, Munitions and Chemical Command ATTN: SMCAR-CCS-C, T Hung Picatinny Arsenal, NJ 07806-5000
1	Commandant US Army Field Artillery School ATTN: ATSF-CMW Ft Sill, OK 73503
1	Commandant US Army Armor Center ATTN: ATSB-CD-MLD Ft Knox, KY 40121
1	Commander US Army Development and Employment Agency ATTN: MODE-TED-SAB Fort Lewis, WA 98433
1	Commander Naval Surface Weapons Center ATTN: D.A. Wilson, Code G31 Dahlgren, VA 22448-5000
1	Commander Naval Surface Weapons Center ATTN: Code G33, J. East Dahlgren, VA 22448-5000

DISTRIBUTION LIST

No. of Copies	Organization
2	Commander US Naval Surface Weapons Ctr ATTN: O. Dengel K. Thorsted Silver Spring, MD 20902-5000
1	Commander Naval Weapons Center China Lake, CA 93555-6001
1	Commander Naval Ordnance Station ATTN: C. Dale Code 5251 Indian Head, MD 20640
1	Superintendent Naval Postgraduate School Dept of Mechanical Engr ATTN: Code 1424, Library Monterey, CA 93943
1	AFWL/SUL Kirtland AFB, NM 87117
1	Air Force Armament Lab ATTN: AFATL/DLODL Eglin AFB, FL 32542-5000
1	AFOSR/NA (L. Caveny) Bldg 410 Bolling AFB, DC 20332
1	Commandant USAFAS ATTN: ATSF-TSM-CN Ft Sill, OK 73503-5600
1	US Bureau of Mines ATTN: R.A. Watson 4800 Forbes Street Pittsburgh, PA 15213
1	Director Jet Propulsion Lab ATTN: Tech Library 4800 Oak Grove Drive Pasadena, CA 91109
2	Director National Aeronautics and Space Administration ATTN: MS-603, Tech Lib MS-86, Dr. Povinelli 21000 Brookpark Road Lewis Research Center Cleveland, OH 44135
1	Director National Aeronautics and Space Administration Manned Spacecraft Center Houston, TX 77058
10	Central Intelligence Agency Office of Central Reference Dissemination Branch Room GE-47 HQS Washington, DC 20502
1	Central Intelligence Agency ATTN: Joseph E. Backofen HQ Room 5F22 Washington, DC 20505
3	Bell Aerospace Textron ATTN: F. Boorady F. Picirillo A.J. Friona PO Box One Buffalo, NY 14240
1	Calspan Corporation ATTN: Tech Library PO Box 400 Buffalo, NY 14225

DISTRIBUTION LIST

No. of Copies	Organization
7	General Electric Ord Sys Div ATTN: J. Mandzy, OP43-220 R.E. Mayer H. West M. Bulman R. Pate I. Magoon J. Scudiere 100 Plastics Avenue Pittsfield, MA 01201-3698
1	General Electric Company Armament Systems Department ATTN: D. Maher Burlington, VT 05401
1	IITRI ATTN: Library 10 W. 35th St Chicago, IL 60616
1	Morton Thiokol Corp Elkton Division ATTN: Dr. R. Biddle Elkton, MD 21921
1	Olin Chemicals Research ATTN: David Gavin PO Box 586 Chesire, CT 06410-0586
2	Olin Corporation ATTN: Victor A. Corso Dr. Ronald L. Dotson PO Box 30-9644 New Haven, CT 06536
1	Paul Gough Associates ATTN: Paul Gough PO Box 1614 Portsmouth, NH 03801
1	Safety Consulting Engr ATTN: Mr. C. James Dahn 5240 Pearl St Rosemont, IL 60018
1	Science Applications, Inc. ATTN: R. Edelman 23146 Cumorah Crest Woodland Hills, CA 91364
2	Sundstrand Aviation Operations ATTN: Mr. Owen Briles Mr. L. Joesten PO Box 7202 Rockford, IL 61125
1	Veritay Technology, Inc. ATTN: E.B. Fisher 4845 Millersport Highway PO Box 305 East Amherst, NY 14051-0305
1	Director Applied Physics Laboratory The Johns Hopkins Univ. Johns Hopkins Road Laurel, MD 20707
2	Director CPIA The Johns Hopkins Univ. ATTN: T. Christian Tech Library Johns Hopkins Road Laurel, MD 20707
1	The Johns Hopkins Univ. ATTN: Prof. W.S. Koski Department of Chemistry Baltimore, MD 21218

DISTRIBUTION LIST

No. of Copies	Organization
1	U. of Illinois at Chicago ATTN: Professor Sohail Murad Dept of Chemical Engr Box 4348 Chicago, IL 60680
1	U. of MD at College Park ATTN: Professor Franz Kasler Department of Chemistry College Park, MD 20742
1	U. of Missouri at Columbia ATTN: Professor R. Thompson Department of Chemistry Columbia, MO 65211
1	U. of Michigan ATTN: Prof. Gerard M. Faeth Dept of Aerospace Engr Ann Arbor, MI 48109-3796
1	U. of Missouri at Columbia ATTN: Professor F.K. Ross Research Reactor Columbia, MO 65211
1	U. of Missouri at Kansas City Department of Physics ATTN: Prof. R.D. Murphy 1110 East 48th Street Kansas City, MO 64110-2499
1	Pennsylvania State University Dept of Mechanical Engr ATTN: Prof. K. Kuo University Park, PA 16802
2	Princeton Combustion Rsch Laboratories, Inc. ATTN: N.A. Messina M. Summerfield 475 US Highway One North Monmouth Junction, NJ 08852
1	University of Arkansas Dept of Chemical Engr ATTN: J. Havens 227 Engineering Building Fayetteville, AR 72701
3	University of Delaware Department of Chemistry ATTN: Mr. James Cronin Professor Thomas Brill Mr. Peter Spohn Newark, DE 19711

Aberdeen Proving Ground

Dir, USAMSAA
ATTN: AMXSY-D
AMXSY-MP, H. Cohen

Cdr, USATECOM
ATTN: AMSTE-TO-F

Cdr, CRDEC, AMCCOM
ATTN: SMCCR-RSP-A
SMCCR-MU
SMCCR-SPS-IL

USER EVALUATION SHEET/CHANGE OF ADDRESS

This Laboratory undertakes a continuing effort to improve the quality of the reports it publishes. Your comments/answers to the items/questions below will aid us in our efforts.

1. BRL Report Number_____ Date of Report_____

2. Date Report Received_____

3. Does this report satisfy a need? (Comment on purpose, related project, or other area of interest for which the report will be used.)_____

4. How specifically, is the report being used? (Information source, design data, procedure, source of ideas, etc.)_____

5. Has the information in this report led to any quantitative savings as far as man-hours or dollars saved, operating costs avoided or efficiencies achieved, etc? If so, please elaborate._____

6. General Comments. What do you think should be changed to improve future reports? (Indicate changes to organization, technical content, format, etc.)

CURRENT ADDRESS

Name

Organization

Address

City, State, Zip

7. If indicating a Change of Address or Address Correction, please provide the New or Correct Address in Block 6 above and the Old or Incorrect address below.

OLD ADDRESS

Name

Organization

Address

City, State, Zip

(Remove this sheet, fold as indicated, staple or tape closed, and mail.)

FOLD HERE

Director
US Army Ballistic Research Laboratory
ATTN: DRXBR-OD-ST
Aberdeen Proving Ground, MD 21005-5066

NO POSTAGE
NECESSARY
IF MAILED
IN THE
UNITED STATES

OFFICIAL BUSINESS
PENALTY FOR PRIVATE USE, $300

BUSINESS REPLY MAIL
FIRST CLASS PERMIT NO 12062 WASHINGTON, DC
POSTAGE WILL BE PAID BY DEPARTMENT OF THE ARMY

Director
US Army Ballistic Research Laboratory
ATTN: DRXBR-OD-ST
Aberdeen Proving Ground, MD 21005-9989

FOLD HERE